# Superasymmetric two-center shell model for spontaneous heavy-ion emission

M. Mirea
*Institute of Atomic Physics, P.O. Box MG-6, Bucharest, Romania*
(Received 22 August 1995; revised manuscript received 1 February 1996)

The single particle levels for the heavy-ion emission process are computed. This decay mode is treated like a superasymmetric fission process. The nuclear shape parametrization is characterized by three degrees of freedom. The difficulties encountered in the microscopic determination of the energy scheme at these very large mass asymmetries are presented. Thereby, a new version of the two-center model, especially designed for very large mass asymmetries, is described. The $^{14}$C heavy-ion spontaneous emission from the parent nucleus $^{223}$Ra is treated in the frame of this model. The principal trends of the variations obtained for the energetic levels during this superasymmetric nuclear decay are discussed. Mainly, for this kind of decay mode, the levels with lower values of the angular momentum projection $\Omega$ show more pronounced variations than those with higher $\Omega$. Also, a qualitative explanation for the favoring of the first excited states in the fine structure in this radioactive process is given. [S0556-2813(96)01906-1]

PACS number(s): 23.70.+j, 21.60.Cs, 21.60.Gx

## I. INTRODUCTION

In 1980, four theoretical models were published in order to predict, as a new nuclear phenomenon, heavy-ion emission: the fragmentation theory, some penetrability calculations like the traditional theory of $\alpha$ decay, the analytical superasymmetric fission model (ASAFM), and the numerical superasymmetric fission model (NSAFM). Many new decay modes have been predicted: $^{5-7}$Li, $^{7-9}$Be, $^{10-12}$B, $^{12-14}$C, $^{14-16}$N, $^{15-18}$O, $^{19,22}$F, $^{20-25}$Ne, $^{28}$Mg, $^{32,34}$Si, $^{46}$Ar, and $^{48,50}$Ca. Some of these predictions are made by considering that the heavy-ion emission is a very asymmetric fission process. An overview and the main features of these theories can be found in Ref. [1].

In 1984, the experimental detection of the $^{14}$C emission from $^{223}$Ra [2] proved the existence of spontaneous heavy-ion emission and opened a new field of interest. A very small value of the branching ratio relative to $\alpha$ decay is found: $b=(8.5\pm2.5)\times10^{-10}$. Up to now, information about the existence and the lifetime of the next decay modes is available: $^{14}$C from $^{221}$Fr, $^{221-224,226}$Ra, and $^{225}$Ac; $^{20}$O from $^{228}$Th; $^{23}$F from $^{231}$Pa; $^{24}$Ne from $^{231}$Pa, $^{230}$Th, and $^{232-234}$U; $^{28}$Mg from $^{234}$U and $^{236,238}$Pu; $^{32}$Si from $^{238}$Pu; and $^{34}$Si from $^{242}$Cm.

A fine structure in the $^{14}$C radioactivity of $^{223}$Ra was discovered with the magnetic spectrometer SOLENO [3]. The possible existence of this phenomenon was suggested earlier, after the first experiment accomplished in order to confirm this cluster decay mode [4], which used a mass spectrometer. Moreover, the experimental result shows that the transitions to the first excited states of the daughter $^{209}$Pb are favored. This phenomenon can be explained only from a microscopical point of view while most models used in the analysis of heavy-cluster decay are based essentially on Gamow's theory with macroscopic potentials. In this sense, a first attempt was made in calculating the overlap between the reflection-asymmetric ground state of $^{223}$Ra and the spherical shell model orbitals of $^{209}$Pb [5]. Also, consistent data are obtained with the enlarged superfluid model [6]. Some estimations of the hindrance factors for $^{14}$C cluster decays in the translead region have been reported. Major difficulties arise in determining truly microscopically the spectroscopic amplitude leading to a schematization of the model. Nevertheless, the theoretical considerations succeed only partially successfully in explaining the experimental result. Therefore a description of this phenomenon with new assumptions, a new version of the asymmetric two-center shell model, especially designed to account for cluster emission, is attempted. The basic idea is to follow the variations of the levels beginning with the states of the initial parent nucleus up to those of the two final fragments. The nuclear shape parametrization chosen for this purpose is presented in Sec. II. In Sec. III, a detailed description of the superasymmetric two-center shell model (STCSM) is offered. Results obtained in the framework of this model are shown in Sec. IV.

## II. THE NUCLEAR SHAPE PARAMETRIZATION

The nuclear parametrization is defined by smoothly joining two intersecting spheres of radius $R_1$ and $R_2$ with a neck surface generated by the rotation of a circle of radius $R_3$ around the symmetry axis, as presented in Fig. 1. The distance between the center of this circle and the axis of symmetry is given by $\rho_3$. By imposing the condition of volume conservation, the surface is perfectly determined by the values of the parameters $R$ (distance between the centers of the spheres), $R_3$ (the radius of the neck) or $C=S/R_3$ (where $S=+1$ when $\rho_3-R_3\geqslant0$ and $S=-1$ when $\rho_3-R_3<0$), and $R_2$ (the radius of the emitted fragment). These three parameters characterize the elongation, the necking, and the mass asymmetry, respectively. Due to the axial symmetry of this system, the surface equation is given in cylindrical coordinates:

$$\rho_s(z)=\begin{cases}[R_1^2-(z-z_1)^2]^{1/2}, & z\leqslant z_{c1}\\ \rho_3-S[R_3^2-(z-z_3)^2]^{1/2}, & z_{c1}<z<z_{c2}\\ [R_2^2-(z-z_2)^2]^{1/2}, & z\geqslant z_{c2}.\end{cases} \quad (1a)$$

For extremely large values of $R_3$, which means for $C=S/R_3=0$ fm$^{-1}$, the parametrization is described in the interval $z_{c1}<z<z_{c2}$ by the relation

 

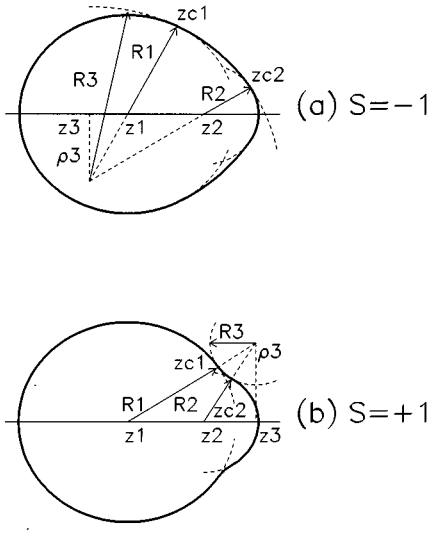


FIG. 1. The nuclear shape parametrization. The case (a) presents the necked shapes characterized by $S=1$ and the case (b) the diamondlike shapes characterized by $S=-1$.

$$\rho_s(z)=[a(z-z_{c1})+b]^{1/2} \tag{1b}$$

with

$$a=\{[R_2^2-(z_{c2}-z_2)^2]^{1/2}-[R_1^2-(z_{c1}-z_1)^2]^{1/2}\}/(z_{c2}-z_{c1}),$$

$$b=[R_1^2-(z_{c1}-z_1)^2]^{1/2}.$$

The significance of all the geometrical symbols can be understood from the Fig. 1. The subscripts 0, 1, and 2 indicate the parent, daughter, and the emitted nuclei, respectively. The initial radius of the parent is $R_0=r_0A_0^{1/3}$, the final radii of the two fragments are $R_{if}=r_0A_i^{1/3}$, with $i=1,2$, and the constant radius $r_0=1.16$ fm. In Eq. (1), $\rho_s$ denotes the value of the coordinate $\rho$ on the nuclear surface. Diamondlike shapes are obtained for $S=-1$ and necked-in shapes for $S=+1$. When $S=-1$, the volume of the emitted fragment, $V_2$, is always computed in the interval $[z_{c2},z_2+R_2]$. In the case $S=+1$ we compute this volume in the interval $[z_{c2},z_2+R_2]$ when $z_{c2}\leqslant z_3$ and in $[z_3,z_2+R_2]$ when $z_{c2}\geqslant z_3$. Throughout the deformation process, the condition of volume conservation $V_1+V_2=V_0$ is preserved. When $R_3=0$ fm, the simple parametrization of two intersecting spheres is obtained. This nuclear shape parametrization has been widely used in nuclear dynamic calculations [7] in a large range of mass asymmetries because it takes into account the most important degrees of freedom encountered in fission processes.

## III. THE SUPERASYMMETRIC TWO-CENTER SHELL MODEL

The theoretical study of fission processes at very large mass asymmetries is limited by the difficulties encountered in the calculations of single particle levels for very deformed one-center potentials. Indeed, on one hand, central potentials are not able to describe in a correct manner the shapes for the passage of one nucleus to two separate nuclei and, on the other hand, for very large prolate deformations the sum of

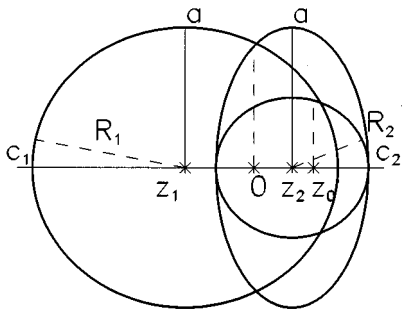


FIG. 2. The nuclear shape parametrization of a sphere intersecting with a spheroid. This parametrization allows analytical solutions for the two-center harmonic potential. The sphere which characterizes the nuclear shape of the light fragment is included in the spheroid.

single particle energies obtained from the level scheme of any smooth potential reaches an infinite value. These difficulties are overcome by considering that the mean field is generated by the nucleons belonging to two nuclear fragments. This dinuclear system can be treated with the two-center shell model [8,9]. This appears to be the simplest method to generalize the Nilsson prescriptions. The two-center shell model is based on the assumption that nucleons can be described in molecular states during the nuclear reaction. This means that the relative motion between the two centers of the potential is slower than the rearrangement of the nucleons in the mean field. This model found a large gamut of uses in various fields like fission or heavy-ion collision processes [10–12] and can be applied to all systems behaving like nuclear molecules [13]. Unfortunately, analytical solutions for the two-center potential are obtained only for semisymmetric shapes as specified in Ref. [14]. This is the principal reason for the failure of the asymmetric two-center shell model in the case of very large mass asymmetries without some improvements. In this work, a new version of the model is presented which is particulary suitable for heavy-ion emission studies.

For the nuclear shape parametrization presented above, the microscopic potential (in cylindrical coordinates) is split, as in Ref. [15], into several parts which are treated separately:

$$V(\rho,z,\varphi)=V_0(\rho,z)+V_{\rm as}(\rho,z)+V_n(\rho,z)+V_{Ls}(\rho,z,\varphi)+V_{L^2}(\rho,z,\varphi)-V_c \tag{2}$$

where $V_0(\rho,z)$ represents the two-center harmonic potential whose eigenvectors can be analytically obtained by solving the Schrödinger equation. It is given by the relation

$$V_0(\rho,z)=\begin{cases}\frac{1}{2}m_0\omega_{z1}^2(z+z_1)^2+\frac{1}{2}m_0\omega_\rho^2\rho^2, & z<0\\ \frac{1}{2}m_0\omega_{z2}^2(z-z_2)^2+\frac{1}{2}m_0\omega_\rho^2\rho^2, & z\geqslant 0,\end{cases} \tag{3}$$

where $m_0$ is the nucleon mass, and $z_1$ and $z_2$ (real, positive) represent the distances between the centers of the spheroids and their intersection plane. From now on, in the following formulas, as a convention, $z_1$ means its absolute value. The calculations are merely simplified by choosing $\omega_{z1}=\omega_\rho=\omega_1$ and $\omega_{z2}=\omega_2$. With this choice, the shape pa-

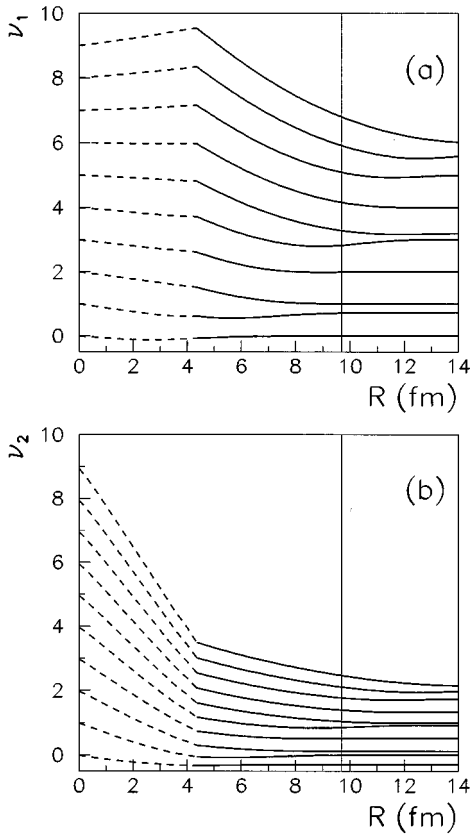


FIG. 3. The variations of the numbers $\nu_1$ (a) and $\nu_2$ (b) with respect to the elongation $R$ in the frame of the two-center potential for the emission of a fragment with mass $A_2=14$ from a parent nucleus with mass $A_0=223$. The dashed line is used to characterize the solutions up to the value $R_i=r_0(A_0^{1/3}-A_2^{1/3})$ which represents the starting configuration of the decay process. A thin line is used to show the touching spheres configuration at the point $R_f=r_0(A_1^{1/3}+A_2^{1/3})$.

rametrization of the potential is reduced to that of a compound system formed by a sphere intersecting with a spheroid. This parametrization is presented in Fig. 2. The origin on the $z$ axis is chosen in the geometrical plane of intersection of the sphere with the spheroid.

The role played by the other terms in the relation (2) (which means $V_{\rm as}$, $V_n$, $V_{Ls}$, $V_{L^2}$, and $V_c$, which are related to the mass asymmetry, to the necking, to the spin orbit coupling, to the $\mathbf{L}^2$ correction, and to the depth of the potential, respectively) will be better explained after the presentation of the analytical solutions of the Schrödinger equation with the potential (3).

### A. Analytical solutions of the Schrödinger equation

The orthogonal system of eigenfunctions used to diagonalize the total Hamiltonian is obtained by solving the Schrödinger equation in cylindrical coordinates:

$$\left[-\frac{\hbar^2}{2m_0}\triangle+V_0(\rho,z)\right]\Psi=E\Psi. \tag{4}$$

The ansatz $\Psi(\rho,z,\varphi)=Z(z)R(\rho)\Phi(\varphi)$ leads to the next solutions for the eigenvectors [14] expressed with the aid of the Hermite function [16]:

$$\Phi(\varphi)=\frac{1}{\sqrt{2\pi}}\exp(im\varphi), \tag{5}$$

$$R_{nm}(\rho)=\sqrt{\frac{2}{n!(n+|m|)!}}\alpha_1\exp\left(-\frac{\alpha_1^2\rho^2}{2}\right)\times(\alpha_1\rho)^{|m|}L_n^{|m|}(\alpha_1^2\rho^2), \tag{6}$$

$$Z_\nu(z)=\begin{cases}C_{\nu_1}\exp\left(-\dfrac{\alpha_1^2(z+z_1)^2}{2}\right)\mathcal{H}_{\nu_1}(-\alpha_1(z+z_1)), & z<0\\ C_{\nu_2}\exp\left(-\dfrac{\alpha_2^2(z-z_2)^2}{2}\right)\mathcal{H}_{\nu_2}(\alpha_2(z-z_2)), & z\geqslant 0,\end{cases} \tag{7}$$

where $L_n^m(x)$ is the Laguerre polynomial,

$$\mathcal{H}_\nu(\xi)=\frac{2^\nu\Gamma\left(\frac{1}{2}\right)}{\Gamma[(1-\nu)/2]}F\left(-\frac{\nu}{2},\frac{1}{2};\xi^2\right)+\frac{2^\nu\Gamma(-1/2)}{\Gamma(-\nu/2)}\xi F\left(\frac{1-\nu}{2},\frac{3}{2};\xi^2\right) \tag{8}$$

is the Hermite function expressed in term of the hypergeometric degenerate function,

$$\alpha_i=\sqrt{\frac{m_0\omega_i}{\hbar}},\quad i=1,2, \tag{9}$$

is a length parameter and $C_{\nu_i}$ $(i=1,2)$ represent the normalization constants. The value of the oscillator frequency for the initial parent nucleus is obtained with the well known formula [17] $\hbar\omega_0=41A_0^{-1/3}$. During the disintegration process, the oscillator stiffness is modified using the relation $\omega_i=(R_0/R_i)\omega_0$ $(i=1,2)$. The numerical values of the quantum numbers $\nu_1,\nu_2$ and the normalization constants $C_{\nu_1},C_{\nu_2}$ are obtained from the continuity conditions of the eigenfunctions and their derivatives at $z=0$, together with the normalization and the stationarity conditions:

$$Z_\nu(z)\Big|_{\substack{z\to 0\\ z<0}}=Z_\nu(z)\Big|_{\substack{z\to 0\\ z>0}}, \tag{10}$$

$$\frac{\partial Z_\nu(z)}{\partial z}\Bigg|_{\substack{z\to 0\\ z<0}}=\frac{\partial Z_\nu(z)}{\partial z}\Bigg|_{\substack{z\to 0\\ z>0}}, \tag{11}$$

$$\int_{-\infty}^{\infty}|Z_\nu(z)|^2dz=1, \tag{12}$$

$$\hbar\omega_1\left(\nu_1+\frac{1}{2}\right)=\hbar\omega_2\left(\nu_2+\frac{1}{2}\right). \tag{13}$$

To go further, it is necessary to locate the levels with a given quantum number asymptotically in the first or in the second potential well. This problem can be reduced to the

knowledge of the variations of the values $\nu_1$ and $\nu_2$ when the elongation tends to infinity. Asymptotically, one of these two values becomes an integer, and the other remains real. Indeed, if $\lim_{z_1\to\infty}\nu_1=n_{z1}=$ integer, then $\lim_{z_2\to\infty}\nu_2=(\omega_2/\omega_1)(n_{z1}+\frac{1}{2})-\frac{1}{2}$, $\lim_{z_1\to\infty}C_{\nu_1}=(2^{n_{z1}}n_{z1}!\pi^{1/2}\alpha_1)^{1/2}$, and $\lim_{z_2\to\infty}C_{\nu_2}=0$. Also, if $\lim_{z_2\to\infty}\nu_2=n_{z2}=$ integer, then $\lim_{z_1\to\infty}\nu_1=(\omega_1/\omega_2)(n_{z2}+\frac{1}{2})-\frac{1}{2}$, $\lim_{z_2\to\infty}C_{\nu_2}=(2^{n_{z2}}n_{z2}!\pi^{1/2}\alpha_2)^{1/2}$, and $\lim_{z_1\to\infty}C_{\nu_1}=0$. For low mass asymmetry, if $n_z$ denotes the initial value of $\nu_1$ and $\nu_2$, then $n_{z1}=n_z/2$ for even $n_z$ values and $n_{z2}=(n_z-1)/2$ for odd $n_z$ values. In the general case, for all possible values of the mass asymmtry, the procedure is a bit more complicated. The first step is to compute the two sequences $n_{z1}^{1i}=i/2$ and $n_{z1}^{2i}=(\omega_1/\omega_2)(i+\frac{1}{2})-\frac{1}{2}$ for $i=0,1,2,\ldots,n_z$. After that, the two sequences are rearranged together in ascending order. The $n_z$th value of this mixed sequence is the limit of $\nu_1$ when $z_1$ tends to infinity. If this value is an integer, that means the level will be located in the first potential well. Otherwise, it will be located in the second potential well. The behavior of the solutions $\nu_1$ and $\nu_2$ with respect to the distance between the centers is shown in Fig. 3 for a very asymmetric case.

The normalization constants are computed using the formulas

$$C_{\nu_2}=\left[\frac{j(\nu_2,\nu_2,\alpha_2 z_2)}{\alpha_2}+\frac{\exp(-\alpha_2^2z_2^2)\mathcal{H}_{\nu_2}^2(-\alpha_2z_2)}{\exp(-\alpha_1^2z_1^2)\mathcal{H}_{\nu_1}^2(-\alpha_1z_1)}\frac{j(\nu_1,\nu_1,\alpha_1z_1)}{\alpha_1}\right]^{-1/2} \tag{14}$$

$$C_{\nu 1}=C_{\nu_2}\frac{\exp(-\alpha_2^2z_2^2/2)\mathcal{H}_{\nu_2}(-\alpha_2z_2)}{\exp(-\alpha_1^2z_1^2/2)\mathcal{H}_{\nu_1}(-\alpha_1z_1)}, \tag{15}$$

where a short notation is used for the integral

$$j(\nu',\nu,\xi_0)=\int_{\xi_0}^{\infty}e^{-\xi^2}\mathcal{H}_{\nu'}(\xi)\mathcal{H}_{\nu}(\xi)d\xi. \tag{16}$$

Numerically, the values of this function can be computed using the relation

$$j(\nu',\nu,\xi_0)=\begin{cases}\dfrac{e^{-\xi_0^2}}{\nu'-\nu}[\nu'\mathcal{H}_{\nu'-1}(-\xi_0)\mathcal{H}_{\nu}(-\xi_0)-\nu\mathcal{H}_{\nu'}(-\xi_0)\mathcal{H}_{\nu-1}(-\xi_0)], & \nu'\neq\nu\\ \dfrac{e^{-\xi_0^2}}{4\Gamma(-\nu)}\left\{\nu\mathcal{H}_{\nu-1}(-\xi_0)\displaystyle\sum_{m=0}^{\infty}\left[(-1)^m\frac{\Gamma[(m-\nu)/2]\psi[(m-\nu)/2]}{m!}(-2\xi_0)^m\right]\right.\\ \quad\left.+\mathcal{H}_{\nu}(-\xi_0)\displaystyle\sum_{m=0}^{\infty}\left[(-1)^m\frac{\Gamma[(m-\nu+1)/2]\psi[(m-\nu+1)/2]}{m!}(-2\xi_0)^m\right]\right\}, & \nu'=\nu\neq\text{integer}\\ e^{-\xi_0^2}\displaystyle\sum_{m=0}^{n-1}\left[2^m\frac{n!}{(n-1)!}H_{n-m+1}(-\xi_0)H_{n-m}(-\xi_0)\right]+2^{n-1}n!\sqrt{\pi}[1+\text{erf}(\xi_0)], & \nu'=\nu=n=\text{integer},\end{cases} \tag{17}$$

where $\text{erf}(\xi)$ is the error function, $H_n(\xi)$ is the Hermite polynomial, and $\psi(\nu)=\Gamma'(\nu)/\Gamma(\nu)$ is the psi function.

The eigenvalues of the potential $V_0$ are

$$\begin{aligned}E_{\nu,n,m}^0&=\hbar\omega_1\left(2n+|m|+\nu_1+\frac{3}{2}\right)\\&=\hbar\omega_2\left(\nu_2+\frac{1}{2}\right)+\hbar\omega_1(2n+|m|+1).\end{aligned} \tag{18}$$

From now on, all the matrix elements of any term of the total Hamiltonian are computed using the system of eigenvectors given by the relations (5)–(7).

### B. The total Hamiltonian

In the total Hamiltonian (2) $V_{\text{as}}$ represents the term which produces a correction of the energy level according to the mass asymmetry. A relation for a potential relative to this term which obviously reproduces the correct single particle levels of two distinct nuclei with spherical shapes, separated at infinity and with very different mass numbers, consists in a compound of two oscillators:

$$V_{\text{as}}^0(\rho,z)=\begin{cases}\frac{1}{2}m_0\omega_1^2(z+z_1)^2+\frac{1}{2}m_0\omega_1^2\rho^2, & z<z_0'\\ \frac{1}{2}m_0\omega_2^2(z-z_2)^2+\frac{1}{2}m_0\omega_2^2\rho^2, & z\geqslant z_0',\end{cases} \tag{19}$$

where $z_0'$ defines the intersection plane of the two distinct potentials characterized by $\omega_1=\omega_{z1}$ and $\omega_2=\omega_{z2}$. This potential is constant on the nuclear surface defined by the parametrization of two intersecting spheres, being always equal to $\frac{1}{2}m_0\omega_1^2R_1^2=\frac{1}{2}m_0\omega_2^2R_2^2$. Let $\rho_{\text{spheres}}(z)$ be the shape equation for this simple dinuclear system with the symbols de-

picted in Fig. 1. Some rapid calculations show that in the $(\rho,z_0')$ plane of intersection of the two spheres, a discontinuity which depends on $\rho$ is present (excepting $\rho=\rho_{\text{spheres}}$):

$$V_{\text{cut}}=\frac{1}{2}m_0(\omega_1^2-\omega_2^2)[\rho^2-\rho^2_{\text{spheres}}(z_0')] = V^0_{as}(\rho,z)\Big|_{\substack{z<z_0'\\ z\to z_0'}} - V^0_{as}(\rho,z)\Big|_{\substack{z>z_0'\\ z\to z_0'}} \tag{20}$$

The interpretation of the formula is easier taking into consideration the equality $\rho_{\text{spheres}}(z_0')=\rho_3$ available for this special configuration. However, even in the case of a potential with a finite number of discontinuities the Schrödinger equation could be solved. The problem resides in the fact that, if the difference $V^0_{as}(\rho,z)-V_0(\rho,z)$ together with the reference potential $V_0(\rho,z)$ are diagonalized directly, the asymptotic levels are not correctly obtained. This difficulty could be overcome resorting separately to two special cases that characterize the inital point of the fission process and the scission point. First, a sphere of radius $R_2$ emerges from the initial spherical parent nucleus of radius $R_0=R_1$, as depicted in Fig. 4. This configuration treats exactly the starting point of the disintegration process. The initial value of the elongation is denoted $R_i=R_0-R_2$ and corresponds to two overlapping tangent spheres. At this moment, a dramatic change is produced in the interval $[z_0',\infty)$ from the value of the potential that characterizes the initial parent nucleus to that determined by the compound system of overlapping spheres. To illustrate this behavior, let $V_1(\rho,z)$ be the potential of the initial spherical parent nucleus and $V_2(\rho,z)$ be that defined by the system at the beginning of the fission process (i.e., the light fragment starts to emerge):

$$V_1(\rho,z)=\tfrac{1}{2}m_0\omega_1^2(z+z_1)^2+\tfrac{1}{2}m_0\omega_1^2\rho^2, \tag{21a}$$

$$V_2(\rho,z)=\begin{cases}\tfrac{1}{2}m_0\omega_1^2(z+z_1)^2+\tfrac{1}{2}m_0\omega_1^2\rho^2, & z<R_1-z_1\\ \tfrac{1}{2}m_0\omega_2^2(z-z_2)^2+\tfrac{1}{2}m_0\omega_2^2\rho^2, & z\geqslant R_1-z_1.\end{cases} \tag{21b}$$

For this configuration the next equality is achieved: $z_0'=R_1-z_1=R_2+z_2$ [with the convention mentioned for the relation (3) that $z_1$ denotes its absolute value]. Consequently, the superasymmetric two-center potential fails to reproduce the level scheme of the spherical oscillator without a supplementary approximation. Denoting by $\Delta E_{01}(z)=V_1(\rho,z)-V_0(\rho,z)$ the quantity obtained on subtracting $V_0(\rho,z)$ [the reference potential given by the relation (3)] from $V_1(\rho,z)$, it is easy to verify that in the $z$-axis region $(-\infty,0]$ the difference $\Delta E_{01}(z)=0$, while in the regions $(0,z_0')$ and $[z_0',\infty)$ the difference is given by the expression $\Delta E_{01}(z)=\frac{1}{2}m_0\omega_1^2(z+z_1)^2-\frac{1}{2}m_0\omega_2^2(z-z_2)^2$. On the other hand, if the subtraction $\Delta E_{\text{as0}}(\rho=0,z)=V^0_{\text{as}}(\rho=0,z)-V_0(\rho=0,z)$ is computed for the $z$-dependent part of the potential, another result is found in the region $[z_0',\infty)$, namely, $\Delta E_{\text{as0}}(\rho=0,z)$ is zero. So the term $\Delta E_{01}$ defined in the interval $[z_0',\infty)$ has significance only at the beginning of the process (for elongations in the vicinity of $R_i$), and after that it must vanish. That could be realized, in a simple way, by imposing a geometrical dependence of the value of this term with respect to some shape parameters. In the following, a linear dependence on $R$ (elongation) is used. Without doubt, this is not the unique way; other kinds of approximations could be used. Therefore, in order to avoid a sharp variation of the single particle energies for this system of overlapping touching spheres, we must use the following partial correction available only at the beginning of the fission process:

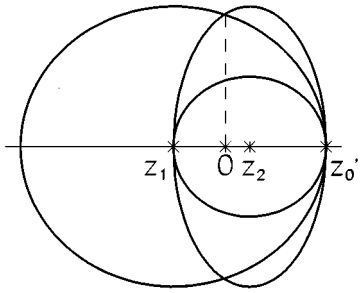


FIG. 4. The nuclear shape parametrization of the system of intersecting sphere and spheroid at the initial moment of the fission process. The nascent light fragment is completely overlapping on the parent nucleus.

$$E_{1c}=\begin{cases}\dfrac{1}{2}m_0\omega_1^2(z+z_1)^2-\dfrac{1}{2}m_0\omega_2^2(z-z_2)^2, & 0<z<z_0'\\ \left[\dfrac{1}{2}m_0\omega_1^2(z+z_1)^2-\dfrac{1}{2}m_0\omega_2^2(z-z_2)^2\right]\left[1-\dfrac{R-R_i}{R_f-R_i}\right], & z\geqslant z_0', R\leqslant R_f\\ 0, & R>R_f.\end{cases} \tag{22}$$

Here, $R_f=R_{1f}+R_{2f}$ denotes the elongation for the compound system of two external tangent spheres, $R_{1f}$ and $R_{2f}$ being, as defined before, the final radius of the daughter and that of the emitted nucleus, respectively. It must be pointed out that for $R>R_f$ the term $E_{1c}$ vanishes in both regions $[0,z_0')$ (because the equality $z_0'=0$ is reached) and $[z_0',\infty)$ (due to the geometrical dependence).

Secondly, let us see the behavior of the limiting case ofthe system formed by two spheres separated at infinity. Obviously, the expected level scheme of such a system must be

the overlap of both the oscillator levels. Moreover, the eigenvalues of the asymmetric two-center shell potential must give for the well of the light fragment the following values:

$$E_{\nu_2 nm}=\hbar\omega_2(\nu_2+2n+|m|+\tfrac{3}{2}). \tag{23}$$

But, in the case of a potential obtained by the intersection of a sphere with a spheroid, according to the relation (19), the asymmetric two-center potential gives the values $E^0_{\nu nm}$. The unique way which allows the modification of the levels with exactly the value $E_{\nu_2 nm}-E^0_{\nu nm}$ after a proper diagonalization in the eigenvector basis of the $V_0$ potential is to define a term of the form

$$E_{2c}(\rho)=m_0\omega_1(\omega_2-\omega_1)\rho^2, \quad z\geqslant z_0', \tag{24}$$

in order to obtain in the final stage of the process

$$\begin{aligned}\langle n'_{z2},n',m'|E_{2c}(\rho)|n_{z2},n,m\rangle &=\hbar(\omega_2-\omega_1)\{(2n+|m|+1)\delta_{n'n}\\ &\quad-[(n+1)(n+|m|+1)]^{1/2}\delta_{n'n+1}\\ &\quad-[n(n+|m|)]^{1/2}\delta_{n'n-1}\}\delta_{n'_{z2}n_{z2}}\delta_{m'm}.\end{aligned}$$

The off-diagonal parts of this expression with $n'=n\pm1$ or $N'=N\pm2$ (because $N=2n+|m|+n_z$) will not affect the asymptotic results because $N$ becomes a good quantum number. The diagonal term ($n'=n$ or $N'=N$) leads to good values of the energies for the two-level schemes belonging to the two final fragments separated at infinity. The two nuclei, in this asymptotic configuration, have the final radii $R_{1f}$ and $R_{2f}$ which define the two frequencies $\omega_1$ and $\omega_2$. This means that the term given by the relation (24) fulfils the condition of adiabatic volume conservation (i.e., the volume enclosed in an equipotential surface remains constant). At the beginning of the fission process, the introduction of the term (24) has no physical meaning. Therefore a geometrical correction is introduced as in the former case in order to have a progressive vanishing towards the beginning of the decay process. Finally, the term of the Hamiltonian due to the mass asymmetry shows the following behavior [using relations (22) and (24)]:

$$V_{\rm as}(\rho,z)=\begin{cases}E_{1c}(z)+\dfrac{R-R_i}{R_f-R_i}E_{2c}(\rho), & R\leqslant R_f\\ E_{1c}(z)+E_{2c}(\rho), & R>R_f.\end{cases} \tag{25}$$

In Fig. 5 the intersection of the potential energy surface $V_s=V_0+V_{\rm as}$ along the $z$ axis is drawn for different values of the distance between centers.

The third term in the relation (2) is $V_n(\rho,z)$. It takes into account the variation of the potential in the presence of a neck. It is derived using the condition of an equipotential value on the nuclear surface defined geometrically. So the two-center potential for shapes with a neck is written in the form

$$V^0_n(\rho,z)=\begin{cases}\dfrac{1}{2}m_0\omega_1^2(z+z_1)^2+\dfrac{1}{2}m_0\omega_1^2\rho^2, & z\leqslant z_{c1}\\ \dfrac{1}{2}m_0R_1^2\omega_1^2+\dfrac{1}{2}m_0\left[\omega_1^2+(\omega_2^2-\omega_1^2)\dfrac{z-z_{c1}}{z_{c2}-z_{c1}}\right]\{\rho^2-\{\rho_3-S[R_3^2-(z-z_3)^2]^{1/2}\}^2\}, & z_{c1}<z<z_0'\\ \dfrac{1}{2}m_0R_2^2\omega_2^2+\dfrac{1}{2}m_0\left[\omega_2^2+(\omega_1^2-\omega_2^2)\dfrac{z_{c2}-z}{z_{c2}-z_{c1}}\right](\rho^2-\{\rho_3-S[R_3^2-(z-z_3)^2]^{1/2}\}^2), & z_0'\leqslant z<z_{c2}\\ \dfrac{1}{2}m_0\omega_2^2(z-z_2)^2+\dfrac{1}{2}m_0\omega_2^2\rho^2, & z\geqslant z_{c2}.\end{cases} \tag{26}$$

This potential satisfies several conditions. First, on the nuclear surface, the potential is constant and its value equals $\frac{1}{2}m_0\omega_2^2R_2^2=\frac{1}{2}m_0\omega_1^2R_1^2$. This behavior is provided by the fact that the second term of the right side of Eq. (26) in the regions $z_{c1}<z<z_0'$ and $z_0'\leqslant z<z_{c2}$ vanishes when $\rho$ reaches the value $\rho_s$ (corresponding to the surface). Secondly, in the planes of separation defined by the values $z_{c1}$ and $z_{c2}$, a continuity of the potential is reached, which means

$$V^0_n(\rho,z)\big|_{\substack{z_{ci}-z\to0\\ z<z_{ci}}}=V^0_n(\rho,z)\big|_{\substack{z-z_{ci}\to0\\ z>z_{ci}}} \quad \text{for} \quad i=1,2.$$

Thirdly, in the neck region, a linear variation of the $\omega^2$ value is realized from $\omega_1^2$ to $\omega_2^2$ leading to the disappearance of the cut in the potential defined by the relation (20), which means

$$V^0_n(\rho,z)\big|_{\substack{z_0'-z\to0\\ z<z_0'}}=V^0_n(\rho,z)\big|_{\substack{z-z_0'\to0\\ z>z_0'}}.$$

The behavior of this potential is depicted as contour lines in Fig. 6.

For the limit case, when $C=0$ fm$^{-1}$, in the $(z_{c1},z_{c2})$ interval another formula is deduced:

$$\begin{aligned}V^0_n(\rho,z)&=\frac{1}{2}m_0R_1^2\omega_1^2+\frac{1}{2}m_0\left[\omega_1^2+(\omega_2^2-\omega_1^2)\frac{z-z_{c1}}{z_{c2}-z_{c1}}\right]\\ &\quad\times\{\rho^2-[a(z-z_{c1})+b]^2\},\end{aligned} \tag{27}$$

where the parameters $a$ and $b$ are defined in relation (1b).

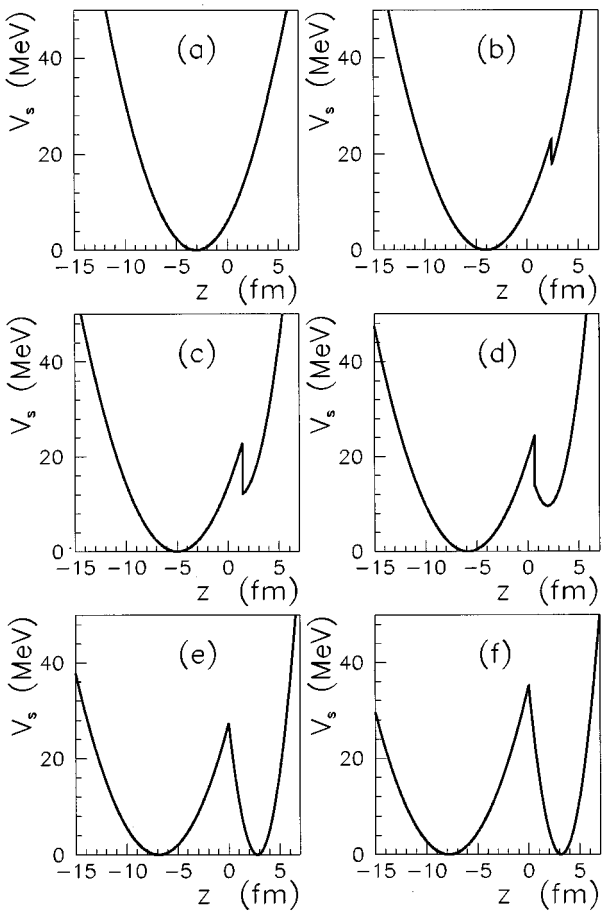


FIG. 5. Intersections of the potential energy surface $V_s = V_0 + V_{as}$ along the $z$ axis for different values of the distance between centers. The normalized coordinate of elongation $R_n = (R - R_i)/(R_f - R_i)$ takes the values 0, 0.25, 0.5, 0.75, 1, and 1.25 for the cases (a), (b), (c), (d), (e), and (f), respectively. The $^{14}$C emission from $^{223}$Ra is treated.

The meaning of the geometrical notations involved in these equations is easy to understand by inspecting Fig. 1. Now a relation for the term in the Hamiltonian which characterizes the variation due to the existence of a neck can be written:

$$V_n(\rho,z) = V_n^0(\rho,z) - V_{as}^0(\rho,z). \tag{28}$$

In this way, a term due to the presence of the neck is introduced in the potential.

Both spin-orbit and $\mathbf{L}^2$ operators were constructed to reproduce the single particle levels which are known for a single sphere and for two spheres separated at an infinite distance. The next formula is deduced for the spin-orbit coupling:

$$V_{Ls}(\rho,z,\varphi) = \begin{cases} \left\{ -\dfrac{\hbar\kappa_1}{m_0\omega_{01}}, \mathbf{Ls} \right\}, & z < z_0' \\ \left\{ -\dfrac{\hbar\kappa_2}{m_0\omega_{02}}, \mathbf{Ls} \right\}, & z \geqslant z_0', \end{cases} \tag{29}$$

where $\{A,B\}$ denotes the anticommutator required for the matrix element symmetrization. The product **Ls** gives

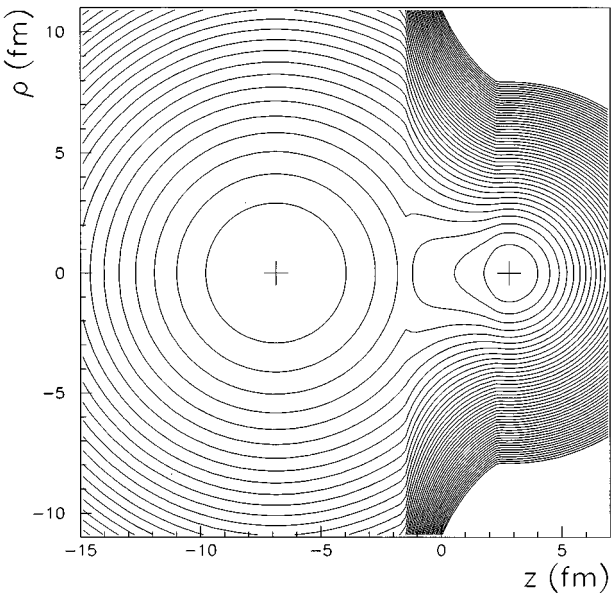


FIG. 6. Contour level values for the potential $V_n^0$. The two centers are marked with crosses. The normalized elongation is $R_n = 1$ and the neck parameter is $R_3 = 4$ fm. The mass asymmetry is the same as for the spontaneous emission of $^{14}$C from $^{223}$Ra. The values of the equipotentials are from 5 to 250 MeV with steps of 5 MeV.

$$\mathbf{Ls} = \tfrac{1}{2}(L^+ s^- + L^- s^+) + L_z s_z \tag{30}$$

with **L** taking a special form adapted for the very asymmetric process:

$$\mathbf{L} = \nabla V^0 \times \mathbf{p}. \tag{31}$$

In this context, the definitions of $V^0$ and $\omega_{0i}$ must reproduce the energetic values of the asymptotic levels for both potential wells. So these quantities are constructed as follows:

$$V^0(\rho,z) = \begin{cases} \tfrac{1}{2}\hbar\omega_1\zeta^2 + \tfrac{1}{2}\hbar\omega_{01}\varrho^2, & z < z_0' \\ \tfrac{1}{2}\hbar\omega_2\zeta^2 + \tfrac{1}{2}\hbar\omega_{02}\varrho^2, & z \geqslant z_0', \end{cases} \tag{32}$$

having a $z$-dependent oscillator frequency

$$\omega_{0i} = \begin{cases} \omega_1, & z < z_0' \\ (\omega_1\omega_2')^{1/2}, & z \geqslant z_0', \end{cases} \tag{33}$$

in terms of the stretched coordinates

$$\zeta = \begin{cases} \alpha_1(z + z_1), & z < z_0' \\ \alpha_2(z - z_2), & z \geqslant z_0', \end{cases} \tag{34}$$

$$\varrho = \alpha_{0i}\rho,$$

and with $\omega_2' = \omega_2 R_0(R_{1f} - R_1)/R_1(R_{1f} - R_0)$ having a variation from $\omega_0$ up to $\omega_2$, in the overlap region of the fragments.

In a similar manner, by imposing the condition to reproduce the asymptotic levels, the $\mathbf{L}^2$ term is found to be

$$V_{L^2}(\rho,z,\varphi)=\begin{cases}\left\{-\frac{1}{2}\frac{\hbar\kappa_1\mu_1}{m_0^2\omega_{01}^2\omega_1},L^2\right\}+\hbar\kappa_1\mu_1\omega_1 N_1\frac{N_1+3}{2}, & z<z_0'\\ \left\{-\frac{1}{2}\frac{\hbar\kappa_2\mu_2}{m_0^2\omega_{02}^2\omega_2'},L^2\right\}+\hbar\kappa_2\mu_2\omega_2' N_2\frac{N_2+3}{2}, & z\geqslant z_0',\end{cases} \tag{35}$$

with

$$\mathbf{L}^2=\frac{1}{2}(L^+L^-+L^-L^+)+L_z^2. \tag{36}$$

According to the existing shell models [8,9,12,14] the variation of the interaction constants for the spin couplings is considered as follows:

$$\kappa_i(i=1,2)=\begin{cases}\kappa_0+(\kappa_i-\kappa_0)\frac{\omega_1-\omega_0}{\omega_{1f}-\omega_0}, & \omega_1<\omega_{1f}\\ \kappa_i, & \omega_1\geqslant\omega_{1f},\end{cases} \tag{37}$$

$$\mu_i(i=1,2)=\begin{cases}\mu_0+(\mu_i-\mu_0)\frac{\omega_1-\omega_0}{\omega_{1f}-\omega_0}, & \omega_1<\omega_{1f}\\ \mu_i, & \omega_1\geqslant\omega_{1f},\end{cases} \tag{38}$$

where $\omega_{1f}=\omega_1 R_1/R_{1f}$. So a gradual variation from the initial to the final state is accounted for by these constants. The procedure to obtain $N_i$ with respect to the elongation is a little more complicated. This value corresponds to the major quantum number for each of two nascent fragments. For the asymmetric two-center shell model, $N$ is no longer a good quantum number. So when the matrix element $\langle\nu',n',m',s'|N_i|\nu,n,m,s\rangle$ is computed, different values for $N_i$ and $N_i'$ must be taken into account. Because these two values do not coincide the following approximation is used:

$$N_i=(N_iN_i')^{1/2}, \tag{39}$$

in which

$$N_i=\begin{cases}N-n_z+n_{zi}+(n_z-n_{zi})\frac{\omega_{1f}-\omega_1}{\omega_{1f}-\omega_0}, & R<R_f\\ N-n_z+n_{zi}, & R\geqslant R_f.\end{cases} \tag{40}$$

Here $n_z$ is an integer representing the quantum number along the $z$ axis for the spherical parent nucleus while $n_{zi}$ $(i=1,2)$ characterize this quantum number for the same level after the asymptotic separation into two fragments.

The last term $V_c$ is a constant which compensates the disadvantage that the harmonic potential gives the single particle levels only up to a constant. In the most general case, we must use three constants for the parent, daughter, and emitted nuclei, respectively. These constants are denoted in the text as $V_{c0}$, $V_{c1}$, and $V_{c2}$, respectively. During the deformation, a variation of these constants in a similar way as described in Eqs. (37) and (38) is followed:

$$V_c(i=1,2)=\begin{cases}V_{c0}+(V_{ci}-V_{c0})\frac{\omega_1-\omega_0}{\omega_{1f}-\omega_0}, & \omega_1<\omega_{1f}\\ V_{ci}, & \omega_1\geqslant\omega_{1f}.\end{cases} \tag{41}$$

It is necessary to point out that $V_{ci}$ is added with respect to $i=1,2$ taking care to identify every level in association with its localization in only one of the two potential wells obtained in the final stage of the process.

The final level scheme is obtained by the diagonalization of the potential (2) with $V_0$, $V_{\rm as}$, $V_n$, $V_{Ls}$, $V_{L^2}$, and $V_c$ given by the formulas (3), (25), (28), (29), (35), and (41), respectively, in the eigenvector basis shown by the relations (5), (6), and (7).

All the interaction constants $\kappa$, $\mu$, and $V_c$ are determined from the relation available for spherical nuclei:

$$E=\hbar\omega\left(N+\frac{3}{2}\right)-\kappa\hbar\omega\left[j(j+1)-l(l+1)-\frac{3}{4}\right]-\kappa\mu\hbar\omega\left(l(l+1)-\frac{N(N+3)}{2}\right)-V_c, \tag{42}$$

where well known notations are used.

### C. The matrix elements

The matrix elements for the term which characterizes the asymmetry are

$$\langle\nu',n',m',s'|V_{\rm as}(\rho,z)|\nu,n,m,s\rangle=\delta_{s's}\delta_{m'm}\frac{m_0}{2}\left(\frac{C_{\nu_2'}C_{\nu_2}}{2}\left\{\omega_1(\omega_2-\omega_1)I_{n'nm}(\rho^2)j(\nu_2',\nu_2,\xi_2-\xi_0')G(R)+\delta_{n'n}\left[\frac{\omega_1^2-\omega_2^2}{\alpha_2^2}[I_{\nu_2',2,\nu_2,\xi_2}-I_{\nu_2',2,\nu_2,(\xi_2-\xi_0')}G(R)]\right.\right.\right.$$
$$\left.\left.\left.+\omega_1^2(z_2+z_1)\left(\frac{2}{\alpha_2}[I_{\nu_2'-1,\nu_2,\xi_2}-I_{\nu_2',1,\nu_2,(\xi_2-\xi_0')}G(R)]+(z_2+z_1)[j(\nu_2',\nu_2,\xi_2)-j(\nu_2',\nu_2,\xi_2-\xi_0')G(R)]\right)\right]\right\}\right) \tag{43}$$

where

$$\xi_2=\alpha_2 z_2, \tag{44}$$

$$\xi_0'=\alpha_2 z_0', \tag{45}$$

$$G(R)=\begin{cases}1, & R>R_f\\ \dfrac{R-R_i}{R_f-R_i}, & R\leqslant R_f,\end{cases} \tag{46}$$

$$I_{\nu',l,\nu,\xi_0}=\int_{\xi_0}^{\infty}e^{\xi^2}\mathcal{H}_{\nu'}(\xi)\xi^l\mathcal{H}_{\nu}(\xi)d\xi$$

$$=-\frac{\xi_0}{2}\exp(-\xi_0^2)\mathcal{H}_{\nu'}(-\xi_0)\xi_0^{l-1}\mathcal{H}_{\nu}(-\xi_0)+\nu' I_{\nu'-1,l-1,\nu,\xi_0}+\nu I_{\nu',l-1,\nu-1,\xi_0}+\frac{l-1}{2}I_{\nu',l-2,\nu,\xi_0}, \tag{47}$$

$$I_{n'nm}(\rho^2)=\int_0^{\infty}R_{n'm}(\rho)\rho^2 R_{nm}(\rho)\rho d\rho$$

$$=\frac{1}{\alpha_1^2}\{(2n+|m|+1)\delta_{n'n}-[(n+1)(n+|m|+1)]^{1/2}\delta_{n'n+1}-[n(n+|m|)]^{1/2}\delta_{n'n-1}\}. \tag{48}$$

Performing the calculations it is useful to remember that $n$ and $m$ are good quantum numbers. The matrix elements of the spin-orbit term are

$$\left\langle \nu',n',m',s'\left|\left\{-\frac{\hbar\kappa}{m_0\omega_{0i}},L_z s_z\right\}\right|\nu,n,m,s\right\rangle=-2\hbar s m\delta_{s's}\delta_{m'm}\delta_{n'n}\Bigg\{m_0\omega_1^2\frac{\hbar\kappa_1}{m_0\omega_{01}}\Bigg[C_{\nu_1'}C_{\nu_1}\frac{j(\nu_1',\nu_1,\xi_1)}{\alpha_1}$$
$$+C_{\nu_2'}C_{\nu_2}\frac{j(\nu_2',\nu_2,\xi_2)-j(\nu_2',\nu_2,\xi_2-\xi_0')}{\alpha_2}\Bigg]$$
$$+m_0\omega_2^2\frac{\hbar\kappa_2}{m_0\omega_2'}C_{\nu_2'}C_{\nu_2}\frac{j(\nu_2',\nu_2,\xi_2-\xi_0')}{\alpha_2}\Bigg\} \tag{49}$$

and

$$\left\langle \nu',n',m',s'\left|\left\{-\frac{\hbar\kappa}{m_0\omega_{0i}},L^+s^-\right\}\right|\nu,n,m,s\right\rangle$$
$$=-\hbar^2\delta_{s',s-1}\delta_{m',m+1}\Bigg\{\Bigg[-m_0\omega_1^2\frac{\hbar\kappa_1}{m_0\omega_{01}}\Bigg(\frac{C_{\nu_1'}C_{\nu_1}}{\alpha_1}[\tfrac{1}{2}j(\nu_1',\nu_1+1,\xi_1)-\nu_1 j(\nu_1',\nu_1-1,\xi_1)-T(\xi_1)]$$
$$+\frac{C_{\nu_2'}C_{\nu_2}}{\alpha_1}\{-\tfrac{1}{2}[j(\nu_2',\nu_2+1,\xi_2)-j(\nu_2',\nu_2+1,\xi_0')]+\nu_2[j(\nu_2',\nu_2-1,\xi_2)-j(\nu_2',\nu_2-1,\xi_0')]+T(\xi_2)-T(\xi_0')\}\Bigg)$$
$$-m_0\omega_2^2\frac{\hbar\kappa_2 C_{\nu_2'}C_{\nu_2}}{m_0\omega_2'\alpha_2}[-\tfrac{1}{2}j(\nu_2',\nu_2+1,\xi_0)+\nu_2 j(\nu_2',\nu_2-1,\xi_0')+T(\xi_0')]\Bigg][(n+|m|+1)^{1/2}\delta_{n',n}-n^{1/2}\delta_{n',n-1}]$$
$$+\Bigg[-m_0\omega_1^2\frac{\hbar\kappa_1}{m_0\omega_{01}}\Bigg(-\frac{C_{\nu_1'}C_{\nu_1}}{\alpha_1}[\tfrac{1}{2}j(\nu_1',\nu_1+1,\xi_1)+\nu_1 j(\nu_1',\nu_1-1,\xi_1)]$$
$$+\frac{C_{\nu_2'}C_{\nu_2}\alpha_1}{\alpha_2^2}\{\tfrac{1}{2}[j(\nu_2',\nu_2+1,\xi_2)-j(\nu_2',\nu_2+1,\xi_0')]+\nu_2[j(\nu_2',\nu_2-1,\xi_2)-j(\nu_2',\nu_2-1,\xi_0')]$$
$$+\alpha_2(|z_1|+z_2)[j(\nu_2',\nu_2,\xi_2)-j(\nu_2',\nu_2,\xi_0')]\}\Bigg)-m_0\omega_2^2\frac{\hbar\kappa_2}{m_0\omega_2'}\frac{C_{\nu_2'}C_{\nu_2}}{\alpha_2}\Bigg[\frac{1}{2}j(\nu_2',\nu_2+1,\xi_0')+\nu_2 j(\nu_2',\nu_2-1,\xi_0')\Bigg]\Bigg]$$
$$\times[(n+|m|+1)^{1/2}\delta_{n',n}+n^{1/2}\delta_{n',n-1}]\Bigg\} \tag{50}$$

where

$$T(\xi)=\frac{\exp(-\xi^2)}{2}\mathcal{H}_{\nu_1'}(-\xi)\mathcal{H}_{\nu_1}(-\xi). \tag{51}$$

The anticomutator needed for the symmetrization of the spin-orbit coupling involves the existence of a Heaviside function. The application of the $\partial/\partial z$ operator on this step function produces finally the terms $T(\xi)$.

To deduce the above formulas the following integrals are also used:

$$\begin{aligned} I_{n'nm}(\rho)&=\int_0^\infty R_{n'm+1}(\rho)\rho R_{nm}(\rho)\rho d\rho \\ &=\frac{1}{\alpha_1}[\delta_{n'n}(n+|m|+1)^{1/2}-\delta_{n'n-1}n^{1/2}] \\ &=I_{n'nm'}(\rho), \end{aligned} \tag{52}$$

$$\begin{aligned} I_{n'nm}(d/d\rho)&=\int_0^\infty R_{n'm+1}(\rho)\frac{d}{d\rho}R_{nm}(\rho)d\rho \\ &=-\alpha_1^2 I_{n'nm}(\rho)+mI_{n'nm}(\rho^{-1}) \\ &\quad -2\alpha_1 n^{1/2}\delta_{n'n-1} \\ &=I_{n'nm'}(d/d\rho), \end{aligned} \tag{53}$$

$$I_{n'nm}(\rho^{-1})=\int_0^\infty R_{n'm+1}(\rho)\rho^{-1}R_{nm}(\rho)\rho d\rho=I_{n'nm'}(\rho^{-1}). \tag{54}$$

The integrals for negative values of the magnetic number are available using the substitution $m'=-|m|-1$ in relations (52)–(54). The factor $\hbar^2$ from the **Ls** expression is contained in $\kappa$.

If the matrix elements of $L^+$ and $L^-$ are known, it is straighforward to obtain the matrix elements of the $\mathbf{L}^2$ interaction using the general relation

$$\langle k'|cO_1O_2|k\rangle=\sum_{k''}\langle k'|c^{1/2}O_1|k''\rangle\langle k''|c^{1/2}O_2|k\rangle \tag{55}$$

where $O_1$ and $O_2$ are two operators and $c$ is a scalar. A generalization of this last relation is used because $c$ can be either negative or positive:

$$\begin{aligned} &\langle \nu',n',m',s'|cL^+L^-|\nu,n,m,s\rangle \\ &=\frac{\delta_{ss'}}{2}\sum_{\nu'',n'',m''}\{\langle \nu',n',m'||c|^{1/2}L^+|\nu'',n'',m''\rangle \\ &\times\langle \nu'',n'',m''|s_g|c|^{1/2}L^-|\nu,n,m\rangle \\ &+\langle \nu',n',m'|s_g|c|^{1/2}L^+|\nu'',n'',m''\rangle \\ &\times\langle \nu'',n'',m''||c|^{1/2}L^-|\nu,n,m\rangle\} \end{aligned} \tag{56}$$

where $s_g=\mathrm{sgn}(c)$.

Let $N_{\mathrm{oc}}$ be the principal quantum number which labels the first occupied level below the Fermi energy. Having in mind that states with $N'=N\pm2$ intervene in the calculations of the matrix elements, that means the cutoff approximation must be done for at least $N_{\max}=N_{\mathrm{oc}}+2$. The truncation effects imply some minor variations at the beginning of the fission process around the true values expected from an adequate spherical potential of the parent nucleus. These are removed with an additional linear fit defined only for the spherical initial shape and which is introduced in the numerical program. Finally, it must be mentioned that the condition of volume conservation is taken into account during the whole process.

## IV. RESULTS AND CONCLUSIONS

The STCSM is used to obtain the energy level diagram of the heavy-ion spontaneous emission of $^{14}$C from the parent nuclide $^{223}$Ra. According to the rule mentioned in Sec. III A which defines the asymptotic quantum numbers with respect to the initial ones, for the cutoff procedure the value $N_{\max}=9$ is chosen.

The values of the spin-orbit and $\mathbf{L}^2$ coupling constants together with those for the depths of the wells are $\kappa=4.837\times10^{-2}$, $\kappa_1=4.979\times10^{-2}$, $\kappa_2=0.217$, $\mu=0.4709$, $\mu_1=0.3959$, and $\mu_2=-0.437$, slightly different from those used in the literature [10,17,18], $V_c=56.67$ MeV, $V_{c1}=55.12$ MeV, and $V_{c2}=54.86$ MeV. The parameters of this two-center potential can be determined by fitting the experimental single particle levels near the Fermi energy for the spherical shapes of the parent, the daughter, and the emitted nuclei (and not for the compound system at an infinite distance as is usually done).

A first look at the results reveals some general behaviors represented in Fig. 7. Here the energetic levels during heavy-ion emission are displayed. A normalized coordinate of the elongation is used, $R_n=(R-R_i)/(R_f-R_i)$. In this example, the nuclear shape parametrization is obtained by the intersection of two spheres, i.e., $R_3=0$ fm. When the normalized elongation takes a zero value, only the single particle states of the spherical parent nucleus $^{223}$Ra are present. Otherwise, for the asymptotic value of the elongation, the superposition of the single particle states for the daughter $^{209}$Pb and the emitted $^{14}$C is recognized. The single particle levels are labeled by their spectroscopic notations on both sides of the picture, adding the superscript $H$ for the heavy fragment and the superscript $L$ for the light one. In Table I the identified final levels are presented together with the corresponding initial values.

In a simple minded interpretation, the heavy-ion emission is somewhat equivalent to forcing some correlated nucleons having small values of the total spin to emerge from the initial nucleus. In the case of $^{14}$C emission, the spins involved are up to $\Omega=3/2$, the occupied shells in their final ground states being $1s^L_{1/2}$, $1p^L_{1/2}$, and $1p^L_{3/2}$. Moreover, it is expected that these removed nucleons have final energies close to the initial values. In Table I, these expectations are accomplished. As an example, $1s^L_{1/2}$ comes from $1f_{7/2}$ and not from $2p_{3/2}$ as the usual asymmetric two-center model model predicts.

At the beginning of the fission process an increase of almost all the energy level values is observed. This trend manifests itself up to a given value of the normalized elongation, which in this case is about 0.3–0.4. Up to this value, it could be considered that the system advances having bulk properties. Afterwards, enlarging the distance between the

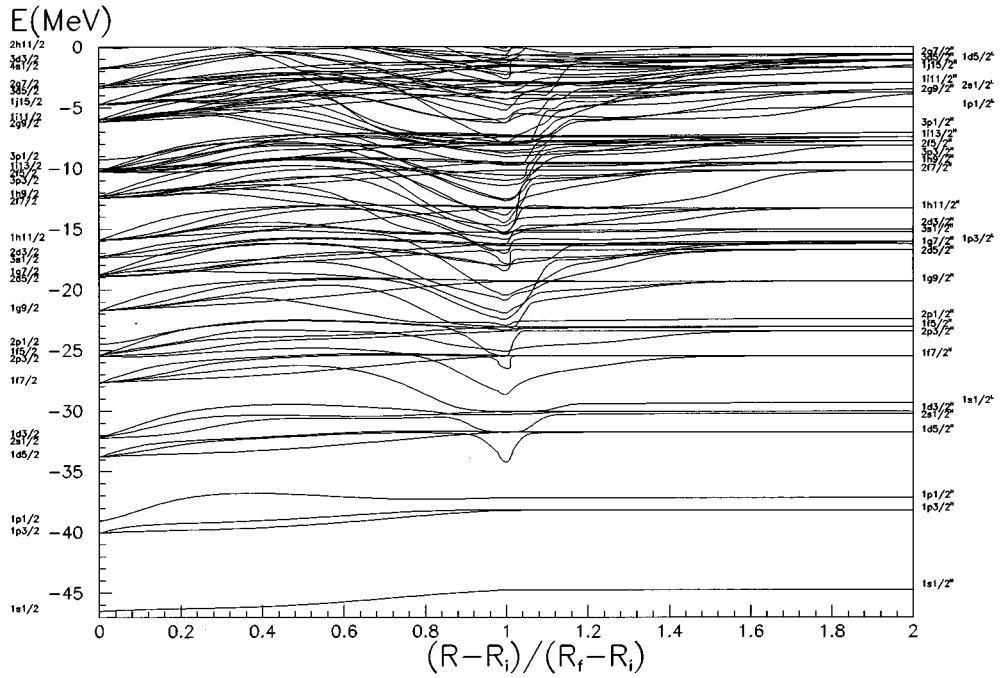


FIG. 7. Level scheme for the $^{14}$C spontaneous emission from $^{223}$Ra with respect to a normalized elongation $(R-R_i)/(R_f-R_i)$, where $R$ is the distance between the centers of the nuclei, $R_i=1.16(A^{1/3}-A_2^{1/3})$ fm is the initial value of the elongation at the beginning of the process, and $R_f=1.16(A_1^{1/3}+A_2^{1/3})$ fm is the elongation at the scission point. The value of $R_3$ is 0 fm.

TABLE I. The levels in the final stage of the disintegration process with respect to their initial values. The spectroscopic notation is used. The levels belonging to $^{209}$Pb have the superscript $H$ (heavy) and those belonging to $^{14}$C have the superscript $L$ (light).

| Initial | Final level with respect to $\Omega$ | | | | | | | |
|---|---|---|---|---|---|---|---|---|
| level | 1/2 | 3/2 | 5/2 | 7/2 | 9/2 | 11/2 | 13/2 | 15/2 |
| $1s1/2$ | $1s1/2^H$ | | | | | | | |
| $1p3/2$ | $1p3/2^H$ | $1p3/2^H$ | | | | | | |
| $1p1/2$ | $1p1/2^H$ | | | | | | | |
| $1d5/2$ | $1d5/2^H$ | $1d5/2^H$ | $1d5/2^H$ | | | | | |
| $1d3/2$ | $1d3/2^H$ | $1d3/2^H$ | | | | | | |
| $1f7/2$ | $1s1/2^L$ | $1f7/2^H$ | $1f7/2^H$ | $1f7/2^H$ | | | | |
| $2p3/2$ | $2f7/2^H$ | $2p3/2^H$ | | | | | | |
| $1f5/2$ | $2p3/2^H$ | $1f5/2^H$ | $1f5/2^H$ | | | | | |
| $2p1/2$ | $1f5/2^H$ | | | | | | | |
| $1g9/2$ | $2p1/2^H$ | $1g9/2^H$ | $1g9/2^H$ | $1g9/2^H$ | $1g9/2^H$ | | | |
| $2d5/2$ | $1g9/2^H$ | $2d5/2^H$ | $2d5/2^H$ | | | | | |
| $1g7/2$ | $2d5/2^H$ | $1p3/2^L$ | $1g7/2^H$ | $1g7/2^H$ | | | | |
| $3s1/2$ | $1p3/2^L$ | | | | | | | |
| $2d3/2$ | $1g7/2^H$ | $1g7/2^H$ | | | | | | |
| $1h11/2$ | $3s1/2^H$ | $2d3/2^H$ | $1h11/2^H$ | $1h11/2^H$ | $1h11/2^H$ | $1h11/2^H$ | | |
| $2f7/2$ | $2d3/2^H$ | $1h11/2^H$ | $2f7/2^H$ | $2f7/2^H$ | | | | |
| $1h9/2$ | $1h11/2^H$ | $2f7/2^H$ | $1h9/2^H$ | $1h9/2^H$ | $1h9/2^H$ | | | |
| $3p3/2$ | $2f7/2^H$ | $1h9/2^H$ | | | | | | |
| $2f5/2$ | $1h9/2^H$ | $3p3/2^H$ | $2f5/2^H$ | | | | | |
| $1i13/2$ | $3p3/2^H$ | $2f5/2^H$ | $1i13/2^H$ | $1i13/2^H$ | $1i13/2^H$ | $1i13/2^H$ | $1i13/2^H$ | |
| $3p1/2$ | $2f5/2^H$ | | | | | | | |
| $2g9/2$ | $1i13/2^H$ | $1i13/2^H$ | $2g9/2^H$ | $2g9/2^H$ | $2g9/2^H$ | | | |
| $1i11/2$ | $3p1/2^H$ | $2g9/2^H$ | $1i11/2^H$ | $1i11/2^H$ | $1i11/2^H$ | $1i11/2^H$ | | |
| $1j15/2$ | $1p1/2^L$ | $1i11/2^H$ | $1j15/2^H$ | $1j15/2^H$ | $1j15/2^H$ | $1j15/2^H$ | $1j15/2^H$ | $1j15/2^H$ |
| $3d5/2$ | $2g9/2^H$ | $1j15/2^H$ | $3d5/2^H$ | | | | | |
| $2g7/2$ | $1i11/2^H$ | $3d5/2^H$ | $2g7/2^H$ | $2g7/2^H$ | | | | |
| $4s1/2$ | $2s1/2^L$ | | | | | | | |
| $3d3/2$ | $1j15/2^H$ | $2g7/2^H$ | | | | | | |

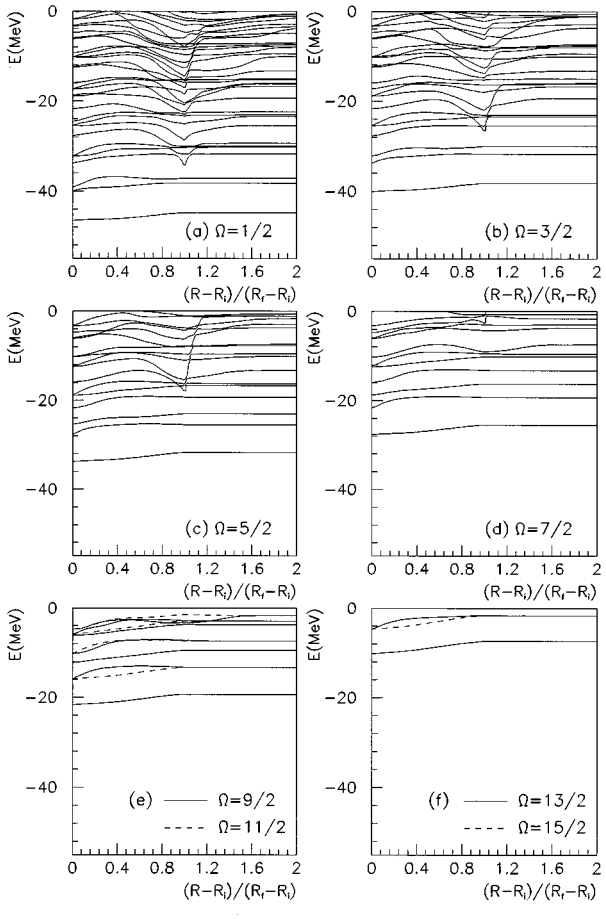


FIG. 8. The levels of Fig. 4 are plotted separately with respect to the projection of the angular momentum. In the cases (a), (b), (c), and (d) levels with the values of $\Omega$ 1/2, 3/2, 5/2, and 7/2 are drawn, respectively. In the case (e) the value of $\Omega=9/2$ is plotted with a full line and 11/2 with a dashed line. In the case (f) the value of $\Omega=13/2$ is ploted with a full line and 15/2 with a dashed line.

two centers, the energetic values of some levels reach in a continuous way the asymptotic final values while the others start to diminish sharply. The decrease in energy of these levels near the scission point leads them below the asymptotic value. This behavior indicates that very asymmetric prolate deformations are very improbable at the beginning of the fission process. Indeed, the deformation energy, regarded as a sum of single particle levels, increases strongly.

Certain energy levels are smoothly behaving whereas other energy levels get more bound in the neighborhood of the touching configuration. This behavior is suggested by the variations of the numbers $\nu_{2i}$ with respect to the elongation [see Fig. 3(b)]. The parametrization used in this context preserves the radius of the emitted fragment ($R_2$) constant. That implies a constant value of $\omega_2$ during the process. So the energy of a given state is directly proportional to $\nu_{2i}$ according to relation (18). In the vicinity of the touching configuration, some numbers $\nu_{2i}$ reach lower values than the same asymptotic ones. For example, this variation achieves a decrease of the energy of about 2 MeV for the levels characterized with the numbers $\nu_{23}$ and $\nu_{24}$. These trends are enhanced after the diagonalization.

A more detailed description of this kind of disintegration is depicted in Fig. 8 where levels with a given projection $|\Omega|$ of the total angular momentum are displayed separately for comparison. Note that a double degeneracy in the angular momentum projection is always present. So, from now on, $\Omega$ will indicate its absolute value. The Nilsson model established as a general rule that on enhancing the prolate deformation, the orbitals with a lower projection of the total spin are displaced toward smaller values of the energy [17]. This rule is no longer valid for the superasymmetric fission process involved here. The levels with the spin projection $\Omega=1/2$ show a more pronounced variation toward high energy values at the beginning of the process. Moreover, for a given projection of the spin, two kinds of behaviors are evidenced. In the lower part of the energetic scheme (which means for levels from shells $1s_{1/2}$, $1p_{3/2}$, and $1p_{1/2}$) the levels present a smooth variation between the initial and the final states. This behavior is no longer seen for the levels existing in the middle part of the energetic diagram, where the proximity of the $1s^L_{1/2}$ level, which will be placed in the second potential well in the final stage of the process, perturbs intensely the other orbitals with the same spin projection. Theoretically, if the asymmetry term $V_{\rm as}$ vanishes, the level $1s^L_{1/2}$ must originate from $1p_{3/2}$. But a rearrangement of the levels shows that the origin of $1s^L_{1/2}$ is $1f_{7/2}$. The Landau-Zener effect (or mutual rejection effect), which avoids the intersection of levels with the same projection of the spin (regarded as a good quantum number), is responsible for this behavior. Also, for $\Omega=1/2$ two levels become almost tangent at $R_n\approx 0.2$ (i.e., $1i_{11/2}$ with $2g_{9/2}$ and $2d_{5/2}$ with $1g_{7/2}$) and another three very pronounced avoided level crossings can be observed at $R_n\approx 0.8$ ($2g_{7/2}$ with $4s_{1/2}$; $2f_{7/2}$ with $1h_{11/2}$; $2d_{3/2}$ with $3s_{1/2}$). For elongations beyond the touching point, the crossings are not important. In Fig. 8(b) the levels with $\Omega=3/2$ are plotted. At $R_n\subset[0.6–0.8]$ three very pronounced avoided level crossings are present ($1i_{11/2}$ with $1j_{15/2}$, $3p_{3/2}$ with $1h_{9/2}$, and $1j_{15/2}$ with $3d_{5/2}$). The levels with energetic values below that of $1f_{7/2}$ reach almost monotonically their final values while a strong variation near the scision point region can be observed for higher levels. In Fig. 8(c) the levels with $\Omega=5/2$ are plotted. At $R_n\approx 0.3$ we find one very pronounced avoided crossing between $1i_{11/2}$ and $1j_{15/2}$. The perturbations, which are understood as very sharp variations in this context, around the scission point begin to be manifested for energies greater than that of the $2d_{5/2}$ level. In Fig. 8(d) the levels with $\Omega=7/2$ are plotted. Here, the perturbations are observed beginning with the $1j_{15/2}$ level. The levels with $\Omega>7/2$ are almost unperturbed and reach their final values continuously.

A numerical analysis accomplished with the two-center potential, which means ignoring the terms $V_{Ls}$ and $V_{L^2}$ in the total Hamiltonian, indicates that the spin interactions are responsible for a strong decrease in energy of the levels belonging to the second potential well around the scision value of the elongation ($R_n\approx 1$). This decrease in energy of the emitted nucleus levels involves variations of the neighboring levels with the same projection of the spin according to the mutual rejection effect. Remembering that, for $R_n>0.5$, at least half of the light fragment volume $V_2$ is already outside the parent nucleus and that the addition of the $\mathbf{L}^2$ term in the Hamiltonian can be partially interpreted as a simulation of a

sudden rise of the potential on the surface, we can therefore interpret the energetic variations around the scision point as surface effects.

Transitions between levels with different spin are improbable for a single nucleon. For an even-odd nucleus, if the system is not excited, the specialization effect [19] explains the energy excess of the nucleus with respect to a given spin of the unpaired nucleon and causes [20] the unfavored transitions which do not follow the Geiger-Nuttal law. The specialization effect fails to describe the experimental transition rates observed in the fine structure of the $^{223}$Ra cluster decay because it considers (adiabatically) the favored transition to the ground state of $^{209}$Pb.

It is possible to explain the experimental result by qualitatively by appealing to the Landau-Zener promotion mechanism, i.e., considering an enhancement of transitions in the region of the avoided level crossings. So, as shown in Table I, for $\Omega = 3/2$, the level $1i_{11/2}$ reaches $2g^H_{9/2}$ asymptotically. But the incoming $1j_{15/2}$ has a first avoided crossing with $1i_{11/2}$ at $R_n \approx 0.5$ and produces the first favored transition of the last nucleon. Another very pronounced avoided crossing is realized at $R_n \approx 0.8$, producing a great probability to have a transition to $3d_{5/2}$. The final levels of the last nucleon could be $2g^H_{9/2}$, as well as $1i^H_{11/2}$ or $1j^H_{15/2}$. It is known that $^{223}$Ra has the spin 3/2 emerging from $1i_{11/2}$. That represents a qualitative explanation for the fine structure in the $^{14}$C radioactivity of $^{223}$Ra. Indeed, the experiment shows that the intensities of the above mentioned transitions are 11% for the Pb ground state $9/2^+$, 81% for the first excited state $11/2^+$ at 0.779 MeV, and 4% for the second excited state $15/2^-$ at 1.423 MeV. Recently [20], new experimental work partially contradicts the previous results, claiming that transitions to the $1j^H_{15/2}$ orbital are hindered. Nevertheless, this schematic description provides some information in understanding the heavy-cluster decay.


[1] D.N. Poenaru and M.S. Ivascu, in *Particle Emission from Nuclei*, edited by D.N. Poenaru and M. Ivascu (CRC Press, Boca Raton, Florida, 1989), Vol. II, Chap. 5, p. 127.

[2] H.J. Rose and G.A. Rose, Nature **307**, 245 (1984).

[3] L. Brillard, A.G. Elayi, E. Hourani, M. Houssonnois, J.F. Le Du, L.H. Rosier, and L. Stab, C. R. Acad. Sci. **309**, 1105 (1989).

[4] W. Henning and W. Kutschera, in *Particle Emission From Nuclei* [1], Vol. II, Chap. 7, p. 203.

[5] R.K. Sheline and I. Ragnarsson, Phys. Rev. C **43**, 1476 (1991).

[6] O. Dumitrescu, in *Frontier Topics in Nuclear Physics*, edited by W. Scheid and A. Sandulescu (Plenum Press, New York, 1994), p. 73.

[7] M. Mirea, D.N. Poenaru, W. Greiner, Z. Phys. A **349**, 39 (1994).

[8] P. Holzer, U. Mosel, and W. Greiner, Nucl. Phys. **A138**, 241 (1969).

[9] D. Scharnweber, W. Greiner, and U. Mosel, Nucl. Phys. **A164**, 257 (1971).

[10] J.Y. Park, W. Greiner, and W. Scheid, Phys. Rev. C **21**, 958 (1980).

[11] J.Y. Park, A. Thiel, W. Scheid, and W. Greiner, in *Frontier Topics in Nuclear Physics* [6], p. 407.

[12] A. Thiel, J. Phys. G **16**, 867 (1990).

[13] W. Greiner, J.Y. Park, and W. Scheid, *Nuclear Molecules* (World Scientific, Singapore, 1995).

[14] J. Maruhn and W. Greiner, Z. Phys. **251**, 431 (1972).

[15] M. Mirea, D.N. Poenaru, and Doina Mirea, Rom. J. Phys. **38**, 71 (1993).

[16] E. Badralexe, M. Rizea, and A. Sandulescu, Rev. Roum. Phys. **19**, 63 (1974).

[17] S.G. Nilsson, C.F. Tsang, A. Sobiczewski, Z. Szymanski, S. Wycech, C. Gustafson, I.L. Lamm, P. Moller, and B. Nilsson, Nucl. Phys. **A131**, 1 (1969).

[18] I. Ragnarson, in Proceedings of the International Conference on Properties of Nuclei Far from the Region of Beta Stability, Leysin, CERN Report No. 1970-30, 1970, p. 847.

[19] J.A. Wheeler in *Niels Bohr and the Development of Physics*, edited by W. Pauli, L. Rosenfeld, and W. Weisskopf (Pergamon Press, London, 1955), p. 163.

[20] E. Hourany, G. Berrier-Ronsin, A. Elayi, P. Hoffmann-Rothe, A.C. Mueller, L. Rosier, G. Rotbard, G. Renou, A. Liebe, D.N. Poenaru, and H.L. Ravn, Phys. Rev. C **52**, 267 (1995).